Using core complex geometry to constrain fault strength

Eunseo Choi,[1] W. Roger Buck,[2] Luc L. Lavier,[3,4] and Kenni Dinesen Petersen[2,5]

Received 3 June 2013; accepted 9 July 2013; published 7 August 2013.

[1] We present the first model results showing that some core complex detachment faults are strong and that their strength has to be in a narrow range to allow certain extensional structures to develop. The structures we simulate are kilometer-scale "rider blocks" that are particularly well observed on some oceanic core complexes as well as continental metamorphic core complexes. Previous numerical simulations of lithospheric extension produced the large-offset, core complex-forming, normal faults only when the faults were weaker than a given threshold. However, our new, high-resolution simulations indicate that rider blocks only result when the faults are stronger than a given level. A narrow range of fault weakening, relative to intact surrounding rock, allows for a consecutive series of rider blocks to emerge in a core complex-like geometry. Our results show that rider blocks develop when the dominant form of weakening is by reduction of fault cohesion while faults that weaken primarily by friction reduction do not form distinct rider blocks.
Citation: Choi, E., W. R. Buck, L. L. Lavier, and K. D. Petersen (2013), Using core complex geometry to constrain fault strength, *Geophys. Res. Lett.*, *40*, 3863–3867, doi:10.1002/grl.50732.

1. Introduction

[2] Faults must be weaker than surrounding rocks to explain observed localization of strain on faults. There is disagreement over just how weak faults are and particularly whether they can be characterized as having normal versus low values of friction. Laboratory measurements indicate that for most rocks, the friction coefficient is between 0.6 and 0.8 [*Byerlee*, 1978] which also predicts relatively high angles for active normal faults formed under subvertical maximum compressive stress, consistent with observed dips of active, seismogenic normal faults that range between ~45° and 60° [*Jackson*, 1987; *Collettini and Sibson*, 2001], and stress differences measured in boreholes [*McGarr and Gay*, 1978; *Brace and Kohlstedt*, 1980; *Townend and Zoback*, 2000].

[3] The recognition of large-offset normal faults, or detachments, in metamorphic core complexes [*Coney*, 1980] that presently dip at a low angle (<30°), or are flat, has been used as an argument that these faults have a very low friction coefficient [e.g., *Hayman et al*., 2003; *Axen*, 2004; *Numelin et al*., 2007]. Several questions about low-angle normal faults are debated including whether they originate with low dips [*Wernicke*, 1981; *Yin*, 1989; *Forsyth*, 1992] or are rotated into that orientation [*Buck*, 1988; *Wernicke and Axen*, 1988]. Some normal faults do appear to be active with a low dip angle, though they may have inherited a low-friction fault zone [*Collettini et al*., 2009]. However, the question of the dip angle for the formation of oceanic detachments has been firmly resolved in favor of high-angle initiation based on the large magnitude of rotation indicated by paleomagnetic studies of drill cores from the footwalls of two oceanic core complexes [*Morris et al*., 2009; *MacLeod et al*., 2011].

[4] Here we consider the implications for fault strength of structures called rider blocks, seen in many continental and oceanic core complexes. Rider blocks are pieces of hanging wall (i.e., from above the fault plane) riding on the master normal fault (Figure 1) of core complexes [*Coney*, 1980; *Rehrig and Reynolds*, 1980; *Davis et al*., 1986; *Reston and Ranero*, 2011]. They were first recognized on continental core complexes (Figure 1a), and recent observations from oceanic core complexes have prompted renewed interest in rider block formation. The initial discovery of oceanic core complexes relied on the mapping of corrugated detachment surfaces that are not covered by rider blocks, but seismic imaging indicates that many oceanic detachments are buried by rider blocks as shown in Figure 1b. Such buried detachments may exist along the as much as half of slow-spreading ridges [*Escartin et al*., 2008; *Reston and Ranero*, 2011] while corrugated surfaces are seen on a much smaller fraction of ridges. Thus, rider blocks may cover vast areas of crust formed at slow-spreading centers [*Reston and Ranero*, 2011].

2. Previous Work

[5] Many core complex detachments are clearly rotated to lower dip angles, or are even overturned, by isostatic adjustment to the topographic loads produced by fault offset [e.g., *Spencer*, 1984]. Models of the regional isostatic response to offset assumed to occur on a single normal fault show that the inactive, upper part of these faults could rotate from initially high dip angle to be nearly flat or overturned as long as the fault offset was greater than the brittle layer thickness. Also, model rider blocks could form if high-angle splay faults periodically grow out of the active faults [e.g., *Buck*, 1988]. These simple models did not consider the range of fault strengths that would explain two questions: (1) How could a single fault develop a very large offset and (2) when would splay faults bounding rider blocks form?

Additional supporting information may be found in the online version of this article.

[1]Center for Earthquake Research and Information, University of Memphis, Memphis, Tennessee, USA.
[2]Lamont-Doherty Earth Observatory, Columbia University, Palisades, New York, USA.
[3]Institute for Geophysics, Jackson School of Geosciences, University of Texas at Austin, Austin, Texas, USA.
[4]Department of Geological Sciences, Jackson School of Geosciences, University of Texas at Austin, Austin, Texas, USA.
[5]Department of Geoscience, Aarhus University, Aarhus, Denmark.

Corresponding author: E. Choi, Center for Earthquake Research and Information, 3890 Central Ave., Memphis, TN 38152, USA. (echoi2@memphis.edu)

0094-8276/13/10.1002/grl.50732

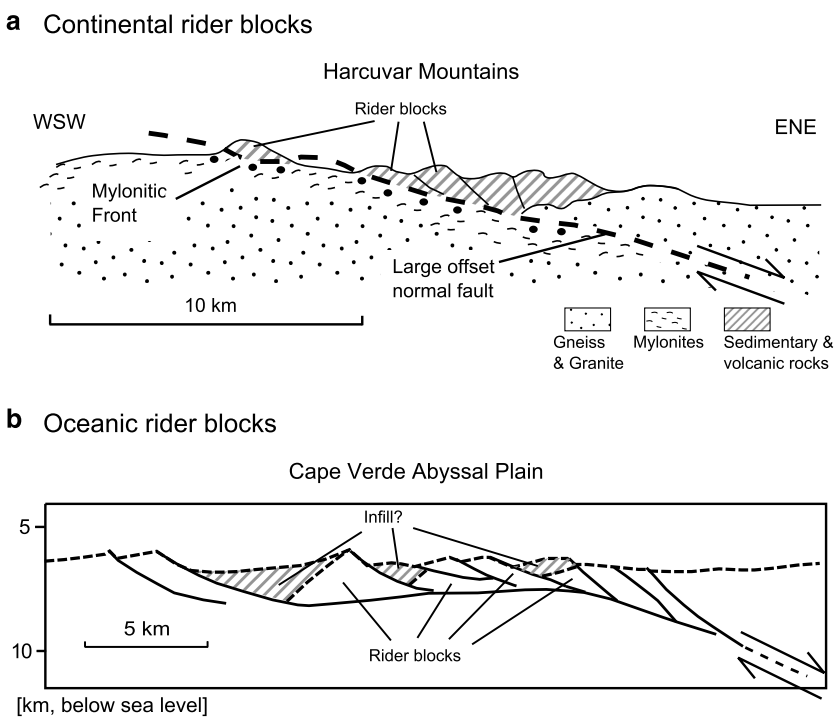

Figure 1. Geometry of rider blocks and the associated master and splay faults. (a) Interpreted cross section of the metamorphic core complex at the Harcuvar Mountains in Arizona, USA. Modified after *Rehrig and Reynolds* [1980]. (b) Structural interpretation of a seismic depth image acquired at the Cape Verde abyssal plain. The dashed lines represent the top of basement or inferred boundaries between basement and infill. Modified after *Reston and Ranero* [2011].

[6] The first of these questions was addressed using analytic and numerical models that came to a somewhat unsurprising conclusion. Namely, for large offset and such large fault rotations to develop, a fault had to be weaker than a given value [e.g., *Forsyth*, 1992; *Buck*, 1993; *Lavier et al*., 2000]. The inactive upper part of such model large-offset faults rotates to domal shapes that compare well to the observed geometry of continental and oceanic core complexes [*Lavier et al*., 1999]. If the fault were too strong, then a series of normal faults develop with no fault accruing sufficient offset to produce the flat faults seen in core complexes.

[7] A theoretical treatment of the second problem [*Choi and Buck*, 2012] suggests that core complex rider blocks only form when the master fault weakening, relative to the surrounding rocks, is in a narrow range. If the fault strength is too low, no rider blocks form since the master fault can slip even if it has rotated to a very low dip. This analysis also predicts that if the fault loses strength primarily by friction reduction, then discrete rider blocks cannot be created. Because the analysis ignored complications, such as changes in stress orientations due to fault offset or partial basin filling, these predictions can only be a rough guide to the conditions needed for rider block formation.

3. Model Formulation

[8] Here we use numerical experiments to investigate the generation of large-offset normal faults and associated rider blocks with a minimum of simplifying assumptions. We follow the numerical procedure employed in some earlier studies of normal fault evolution [*Lavier et al*., 2000] but include two new features essential to simulate rider block development. First, because rider blocks often have dimensions smaller than the brittle layer thickness, the grid spacing needed to resolve them is 5–10 times greater than in earlier studies. Second, the blocks are composed largely of sedimentary and volcanic material that fills the fault-generated basin. Thus, we assume that the basin stays filled up to a depth D_i with respect to the initial surface—a procedure similar to that used in previous studies of effects of sedimentation [e.g., *Burov and Poliakov*, 2001; *Bialas and Buck*, 2009].

[9] We consider extension of an idealized brittle (Mohr-Coulomb) layer as depicted in Figure 2a. The layer floats on an inviscid substratum while the top surface is stress free. Bands of localized plastic strain develop through strain weakening and are considered to represent faults. The process of strain weakening is approximated by reducing cohesion and friction coefficient proportional to the amount of plastic deformation. Previous numerical treatment of fault strain weakening show that results can be made largely independent of mesh size by reducing friction and cohesion as a function of a characteristic amount of fault offset [*Lavier et al*., 2000; *Gerya*, 2013]. We adopt 1.5 km for the characteristic offset in this study, which has been shown to promote large-offset faulting [*Lavier et al*., 2000]. Practically, plastic parameters that are affected by strain weakening are linearly reduced from an initial value to a final value as plastic strain increases to a characteristic value. The characteristic plastic strain is given by the characteristic offset divided by an approximate thickness of shear band (~300 m, 3 times the grid resolution).

[10] The density of the brittle layer is fixed at 2800 kg/m^3. Hydrostatic pore fluid pressures are assumed with a water density (1000 kg/m^3). Material filling in the depression created by fault offset is represented by infill depth (Di) and has the properties as the rest of the brittle layer except the density is 2400 kg/m^3. As inviscid material beneath the brittle

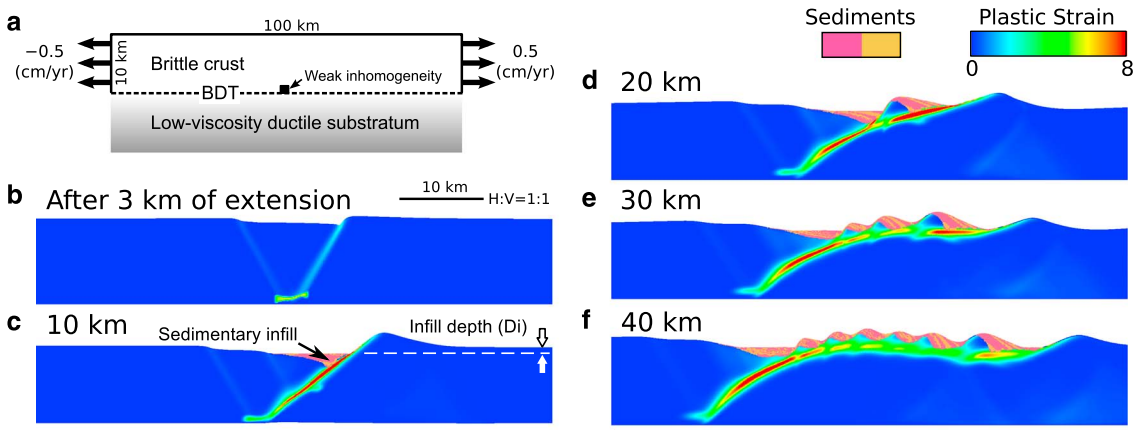

Figure 2. Reference model showing a sequence of rider blocks forming consecutively. (a) Model setup. BDT denotes the brittle-ductile transition. The weak inhomogeneity, slightly off centered to the left, triggers the formation of the first fault. (b–f) Snapshots of accumulated plastic strain and infill distribution with increasing fault offset. Each snapshot shows a 20–80 km extent of the original domain without vertical exaggeration. Lamé's constants are both 30 GPa, $C_i = 20$ MPa, $C_f = 4$ MPa, the initial and final friction coefficients are 0.58, the characteristic offset is 1.5 km, and the densities of crust and infill are 2800 and 2400 kg/m^3, respectively. Infill depth (Di) is a depth from the reference zero level to the top of the infill as visualized in panel C.

layer ascends to 10 km depth, it takes on all properties of that brittle layer as may occur through ductile-to-brittle transition due to hydrothermally assisted cooling [*Lister*, 1980; *Phipps Morgan and Chen*, 1993; *Lavier and Buck*, 2002].

[11] A suite of models were run with different values of parameters such as the initial or final cohesion and the depth of infill. Since previous work shows that a brittle layer thickness around 10 km gives the observed wavelength of doming of core complexes [e.g., *Lavier et al.*, 1999; *Rey et al.*, 2009; *Le Pourhiet et al.*, 2012], the same brittle layer thickness is employed here. The initial friction coefficient is set to be 0.58 but allowed to evolve to different final values through prescribed strain weakening. Values of initial cohesion are in the range of 10–40 MPa, and different final values of cohesion were considered.

4. Results

[12] A case that produced a sequence of sizeable rider blocks is illustrated in Figure 2 (also see the dynamic content Movie S1 in the supporting information). This reference case has an initial cohesion of 20 MPa and an infill depth of 1000 m. The final cohesion is 4 MPa but friction remains unchanged. Snapshots for 3 to 40 km of extension are shown in Figures 2b–2d. The first normal fault to form has a dip of 60°, consistent with the friction coefficient (Figure 2b). As extension proceeds, the footwall is uplifted due to unloading and the master fault bends and rotates. As a result, the fault has a dip of about 45° at 10 km of extension (Figure 2c). With further rotation, the fault locks at depths ≤ ~3 km and a new splay fault forms. Offset of this splay produces a well-defined rider block, composed of the former basin infill and hanging wall crust (Figure 2d). Subsequent rider blocks do not take as long to form because the active master fault around the depth of 3 km remains close to the locking orientation after the first rider block forms. Consequently, their cross-sectional areas are smaller than that of the first block. By extension of 30 km, two more rider blocks are created (Figure 2e) and the system appears capable of producing more rider blocks with continued extension (Figure 2f).

[13] Faulting patterns in our numerical models are sensitive to many parameters such as initial and final cohesion/friction coefficient and infill depth (for an overview, see the supporting information), but we here present some representative cases. For much greater strain weakening than in the reference, model rider blocks do not form. As the initial high-angle normal fault rotates to a low dip at intermediate to shallow depths, it continues to accommodate extension without locking. For an initial cohesion of 20 MPa, final cohesions less than 4 MPa and final friction coefficients less than 0.32 make the initial fault too weak for rider block formation no matter the thickness of infill (Figure 3a). The size of rider blocks depends on fault strength. When a fault is

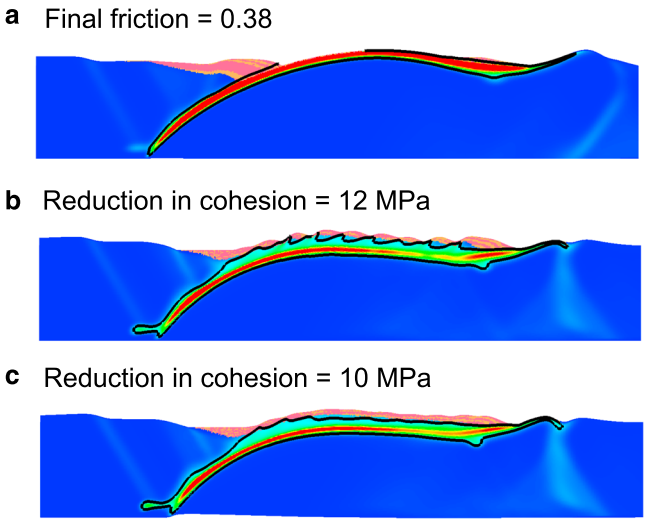

Figure 3. Variations in rider block geometries with different model parameters. Key differences from the reference model (Figure 2) are indicated on top of each model. (a) Lower final friction, 0.38. (b) Higher final cohesion of 8 MPa (reduced by 12 MPa). (c) Even higher final cohesion of 10 MPa (reduced by 10 MPa). The thick black lines in all panels are the contours where plastic strain is 1.75.

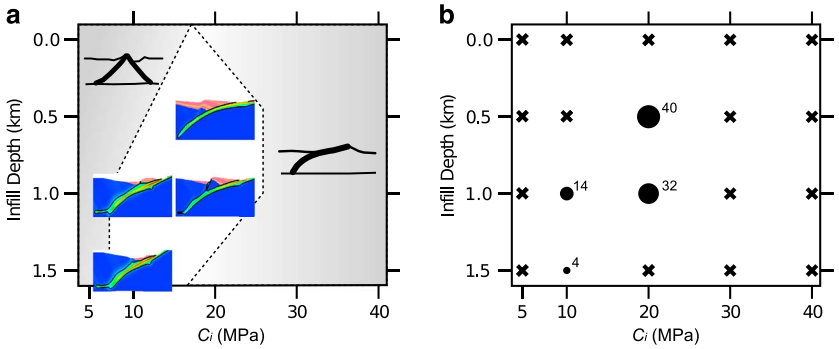

Figure 4. Summary of behaviors of models with total cohesion loss and a constant friction coefficient of 0.58. (a) Images of the first rider blocks, which are centered on the assigned initial cohesion (C_i) and infill depth (D_i). Each image, rendered as in Figure 2, shows a central 20 km wide region of the model domain. The gray-shaded regions (bounded by dashed lines) represent the ranges of C_i and D_i for which rider blocks were not created or disrupted by later-formed faults. Schematic diagrams of the characteristic faulting styles are also shown in the corresponding regions of no rider block in which the thick solid lines represent faults. (b) Phase map showing combinations of C_i and D_i, under which at least one rider block forms and remains intact (solid circles) or none does (crosses). Areas of the solid circles are proportional to the cross-sectional areas of the first-formed rider block in the corresponding models; rider block area is noted next to the circles.

slightly stronger than in the reference model (e.g., the final cohesion equal to 8 MPa), the fault locks after a less amount of rotation as well as at a shallower depth, making the size of and the interval between rider blocks smaller (Figure 3b). A much stronger fault with a final cohesion greater than 10 MPa produces even smaller rider blocks that are difficult to recognize given the current model resolution (Figure 3c).

[14] The effects of variation in cohesion and infill depth on rider block formation are shown in Figure 4a for cases where the fault friction is maintained. The plot shows under what combinations of infill depth and initial cohesion rider blocks can form. Also shown is the cross-sectional area of the first block (Figure 4b). Rider blocks are bigger for greater cohesion loss and for smaller infill depth. This trend is roughly consistent with the prediction by *Choi and Buck* [2012]. However, there is also substantial discrepancy between numerical results and theory in terms of the block sizes as well as the formation conditions. For example, with intermediate amounts of infill (e.g., infill depth ~ 1000 m), rider blocks emerge for a narrower range of cohesion in the analytical treatment compared to the results of this study. The presence of added basin infill changes the stress field, and as a consequence, the shape of the master fault in ways that promote rider block formation. Nevertheless, the range of fault weakening leading to large-offset faults with rider blocks is very restricted. Models considering a wide range of parameters are discussed in the online supporting information.

[15] For models with an initial cohesion of 20 MPa and an infill depth of 1 km (Figures 2 and 3), we find that rider blocks only form when a master fault has a friction coefficient greater than 0.4 and a cohesion reduction between about 12 and 20 MPa. Qualitatively, a rider block-producing fault must have high friction but low final cohesion.

5. Discussion and Summary

[16] Rider blocks generated in our reference model (Figure 2) are reminiscent of the inferred geometry of master and splay faults as well as associated fault blocks seen in continental and oceanic core complexes (Figure 1). However, some core complexes have no rider blocks. Erosion could remove rider blocks in some continental areas though this should not occur for oceanic core complexes. Our results suggest either that the detachments in these complexes have a friction coefficient lower than 0.4 or that the amount of infill is not sufficient to form rider blocks even though friction coefficient is greater than 0.4. In the former case, such low values of friction are consistent with the measured values (< 0.3) for weak minerals like talc found on the corrugated surface [*Escartin et al.*, 1997; *Escartín et al.*, 2003; *Moore et al.*, 2004; *Schroeder and John*, 2004; *Boschi et al.*, 2006; *Karson et al.*, 2006; *Dick et al.*, 2008; *Picazo et al.*, 2012]. The latter case, insufficient infill, has also been suggested as an explanation of the lack of rider blocks on the Atlantis massif, which is located at a volcanic infill-poor ridge-transform intersection [*Reston and Ranero*, 2011].

[17] This is the first study to place upper and lower bounds on the strength of normal faults. Our self-consistent numerical models indicate that large-offset, low-angle normal faults with sizable rider blocks are frictionally strong and have rotated to a low angle from the optimal orientation predicted by Andersonian fault mechanics. Rider blocks emerge with a core complex-like geometry in high-resolution simulations only for a narrow range of fault weakening, relative to intact surrounding rock. Furthermore, they develop when the dominant form of weakening is by reduction of fault cohesion while faults that weaken primarily by friction reduction do not form distinct rider blocks. Our models require that some large-offset faults have values of friction coefficient close to 0.6. Though we have focused on a specific fault type, our results may have implications for faults in general: i.e., faults have "normal" levels of friction, and altered minerals like talc must be present to explain the apparent low-strength features such as core complexes without rider blocks.

[18] **Acknowledgments.** E. Choi and W. R. Buck were partly supported by the U.S. National Science Foundation (NSF) through grant EAR-0911565. E. Choi and L. L. Lavier received partial support from the NSF Continental Dynamics program under grant EAR-0607588. Computations for this study were performed using the HPC resources provided by the Texas Advanced Computing Center at The University of Texas at Austin under TeraGrid grant TG-EAR100019.

[19] The Editor thanks Julia Morgan and an anonymous reviewer for their assistance in evaluating this paper.

References

Axen, G. J. (2004), Mechanics of low-angle normal faults, in *Rheology and Deformation of the Lithosphere at Continental Margins*, edited by G. D. Karner, B. Taylor, N. W. Driscoll, and D. L. Kohlsted, pp. 46–91, Columbia University Press, New York.

Bialas, R. W., and W. R. Buck (2009), How sediment promotes narrow rifting: Application to the Gulf of California, *Tectonics*, *28*, TC4014, doi:10.1029/2008TC002394.

Boschi, C., G. L. Früh-Green, A. Delacour, J. A. Karson, and D. S. Kelley (2006), Mass transfer and fluid flow during detachment faulting and development of an oceanic core complex, Atlantis Massif (MAR 30°N), *Geochem. Geophys. Geosyst.*, *7*, Q01004, doi:10.1029/2005GC001074.

Brace, W. F., and D. L. Kohlstedt (1980), Limits on lithospheric stress imposed by laboratory experiments, *J. Geophys. Res.*, *85*(B11), 6248–6252.

Buck, W. R. (1988), Flexural rotation of normal faults, *Tectonics*, *7*(5), 959, doi:10.1029/TC007i005p00959.

Buck, W. R. (1993), Effect of lithospheric thickness on the formation of high- and low-angle normal faults, *Geology*, *21*, 933–936.

Burov, E., and A. Poliakov (2001), Erosion and rheology controls on synrift and postrift evolution: Verifying old and new ideas using a fully coupled numerical model, *J. Geophys. Res.*, *106*, 16,416–461,481.

Byerlee, J. (1978), Friction of rocks, *Pure Appl. Geophys.*, *116*(4), 615–626.

Choi, E., and W. R. Buck (2012), Constraints on the strength of faults from the geometry of rider blocks in continental and oceanic core complexes, *J. Geophys. Res.*, *117*, B04410, doi:10.1029/2011JB008741.

Collettini, C., and R. H. Sibson (2001), Normal faults, normal friction?, *Geology*, *29*(10), 927–930, doi:10.1130/0091-7613(2001)029<0927:NFNF>2.0.CO;2.

Collettini, C., A. Niemeijer, C. Viti, and C. Marone (2009), Fault zone fabric and fault weakness, *Nature*, *462*(7275), 907–10, doi:10.1038/nature08585.

Coney, P. J. (1980), Cordilleran metamorphic core complexes, in *Cordilleran Metamorphic Core Complexes*, vol. 153, edited by M. D. Crittenden, P. J. Coney, and G. H. Davis, pp. 7–34, GSA Memoir (Geological Society of America), Boulder, Colorado.

Davis, G. A., G. S. Lister, and S. J. Reynolds (1986), Structural evolution of the Whipple and South Mountains shear zones, southwestern United States, *Geology*, *14*(1), 7–10, doi:10.1130/0091-7613(1986)14<7:SEOTWA>2.0.CO;2.

Dick, H. J. B., M. a. Tivey, and B. E. Tucholke (2008), Plutonic foundation of a slow-spreading ridge segment: Oceanic core complex at Kane Megamullion, 23°30′N, 45°20′W, *Geochem. Geophys. Geosyst.*, (9), Q05014, doi:10.1029/2007GC001645.

Escartin, J., G. Hirth, and B. Evans (1997), Nondilatant brittle deformation of serpentinites: Implications for Mohr-Coulomb theory and the strength of faults, *J. Geophys. Res.*, *102*(B2), 2897–2913.

Escartín, J., C. Mével, C. J. MacLeod, and A. M. McCaig (2003), Constraints on deformation conditions and the origin of oceanic detachments: The Mid-Atlantic Ridge core complex at 15°45′N, *Geochem. Geophys. Geosyst.*, *4*(8), 1067, doi:10.1029/2002GC000472.

Escartin, J., D. K. Smith, J. Cann, H. Schouten, C. H. Langmuir, and S. Escrig (2008), Central role of detachment faults in accretion of slow-spreading oceanic lithosphere, *Nature (London)*, *455*(7214), 790–794.

Forsyth, D. (1992), Finite extension and low-angle normal faulting, *Geology*, *20*, 27–30, doi:10.1130/0091-7613(1992)020<0027:FEALAN>2.3.CO;2.

Gerya, T. V. (2013), Three-dimensional thermomechanical modeling of oceanic spreading initiation and evolution, *Phys. Earth Planet. Inter.*, *214*, 35–52, doi:10.1016/j.pepi.2012.10.007.

Hayman, N. W., J. R. Knott, D. S. Cowan, E. Nemser, and A. M. Sarna-Wojcicki (2003), Quaternary low-angle slip on detachment faults in Death Valley, California, *Geology*, *31*(4), 343–346, doi:10.1130/0091-7613(2003)031<0343:QLASOD>2.0.CO;2.

Jackson, J. A. (1987), Active normal faulting and crustal extension, in *Continental Extensional Tectonics*, Geological Society, London, Special Publications, edited by M. P. Coward, J. F. Dewey, and P. L. Hancock, pp. 3–17, Geological Society, London.

Karson, J. A., G. L. Früh-Green, D. S. Kelley, E. A. Williams, D. R. Yoerger, and M. Jakuba (2006), Detachment shear zone of the Atlantis Massif core complex, Mid-Atlantic Ridge, 30°N, *Geochem. Geophys. Geosyst.*, *7*, Q06016, doi:10.1029/2005GC001109.

Lavier, L. L., and W. R. Buck (2002), Half graben versus large-offset low-angle normal fault: Importance of keeping cool during normal faulting, *J. Geophys. Res.*, *107*(B6), 2122, doi:10.1029/2001JB000513.

Lavier, L. L., W. R. Buck, and A. N. B. Poliakov (1999), A self consistent rolling-hinge model for large-offset low-angle normal faults, *Geology*, *24*, 561–564.

Lavier, L. L., W. R. Buck, and A. N. B. Poliakov (2000), Factors controlling normal fault offset in an ideal brittle layer, *J. Geophys. Res.*, *105*(B10), 23,431–23,442, doi:10.1029/2000JB900108.

Le Pourhiet, L., B. Huet, D. A. May, L. Labrousse, and L. Jolivet (2012), Kinematic interpretation of the 3D shapes of metamorphic core complexes, *Geochem. Geophys. Geosyst.*, *13*, Q09002, doi:10.1029/2012GC004271.

Lister, C. R. B. (1980), Heat flow and hydrothermal circulation, *Annu. Rev. Earth Planet. Sci.*, *8*(1), 95–117, doi:10.1146/annurev.ea.08.050180.000523.

MacLeod, C. J., J. Carlut, J. Escartín, H. Horen, and A. Morris (2011), Quantitative constraint on footwall rotations at the 15°45′N oceanic core complex, Mid-Atlantic Ridge: Implications for oceanic detachment fault processes, *Geochem. Geophys. Geosyst.*, *12*, Q0AG03, doi:10.1029/2011GC003503.

McGarr, A., and N. C. Gay (1978), State of stress in the Earth's crust, *Annu. Rev. Earth Planet. Sci.*, *6*(1), 405–436, doi:10.1146/annurev.ea.06.050178.002201.

Moore, D. E., D. A. Lockner, H. Tanaka, and K. Iwata (2004), The coefficient of friction of chrysotile gouge at seismogenic depths, *Int. Geol. Rev.*, *46*(5), 385–398, doi:10.2747/0020-6814.46.5.385.

Morris, A., J. S. Gee, N. Pressling, B. E. John, C. J. MacLeod, C. B. Grimes, and R. C. Searle (2009), Footwall rotation in an oceanic core complex quantified using reoriented Integrated Ocean Drilling Program core samples, *Earth Planet. Sci. Lett.*, 287, 217–228, doi:10.1016/j.epsl.2009.08.007.

Numelin, T., C. Marone, and E. Kirby (2007), Frictional properties of natural fault gouge from a low-angle normal fault, Panamint Valley, California, *Tectonics*, *26*, TC2004, doi:10.1029/2005TC001916.

Phipps Morgan, J., and Y. J. Chen (1993), The genesis of oceanic crust: Magma injection, hydrothermal circulation, and crustal flow, *J. Geophys. Res.*, *98*(B4), 6283–6297.

Picazo, S., M. Cannat, A. Delacour, J. Escartín, S. Rouméjon, and S. Silantyev (2012), Deformation associated with the denudation of mantle-derived rocks at the Mid-Atlantic Ridge 13°–15°N: The role of magmatic injections and hydrothermal alteration, *Geochem. Geophys. Geosyst.*, *13*, Q04G09, doi:10.1029/2012GC004121.

Rehrig, W. A., and S. J. Reynolds (1980), Geologic and geochronologic reconnaissance of a northwest-trending zone of metamorphic core complexes in southern and western Arizona, in *Cordilleran Metamorphic Core Complexes*, vol. 153, edited by M. D. Crittenden, P. J. Coney, and G. H. Davis, pp. 131–156, GSA Memoir (Geological Society of America), Boulder, Colorado.

Reston, T. J., and C. R. Ranero (2011), The 3-D geometry of detachment faulting at mid-ocean ridges, *Geochem. Geophys. Geosyst.*, *12*, Q0AG05, doi:10.1029/2011GC003666.

Rey, P. F., C. Teyssier, and D. L. Whitney (2009), Extension rates, crustal melting, and core complex dynamics, *Geology*, *37*(5), 391–394, doi:10.1130/G25460A.1.

Schroeder, T., and B. E. John (2004), Strain localization on an oceanic detachment fault system, Atlantis Massif, 30°N, Mid-Atlantic Ridge, *Geochem. Geophys. Geosyst.*, *5*, Q11007, doi:10.1029/2004GC000728.

Spencer, J. E. (1984), Role of tectonic denudation in warping and uplift of low-angle normal faults, *Geology*, *12*(2), 95–98, doi:10.1130/0091-7613(1984)12<95:ROTDIW>2.0.CO;2.

Townend, J., and M. D. Zoback (2000), How faulting keeps the crust strong, *Geology*, *28*(5), 399–402, doi:10.1130/0091-7613(2000)28<399:HFKTCS>2.0.CO;2.

Wernicke, B. (1981), Low-angle normal faults in the Basin and Range Province: Nappe tectonics in an extending orogen, *Nature*, *291*, 645–648.

Wernicke, B., and G. J. Axen (1988), On the role of isostasy in the evolution of normal fault systems, *Geology*, *16*(9), 848–851.

Yin, A. (1989), Origin of regional, rooted low-angle normal faults: A mechanical model and its tectonic implications, *Tectonics*, *8*(3), 469–482, doi:10.1029/TC008i003p00469.